



**HAL**  
open science

## Source depth discrimination with a vertical line array

Ewen Conan, Julien Bonnel, Thierry Chonavel, Barbara Nicolas

► **To cite this version:**

Ewen Conan, Julien Bonnel, Thierry Chonavel, Barbara Nicolas. Source depth discrimination with a vertical line array. *Journal of the Acoustical Society of America*, 2016, 140 (5), pp.EL434 - EL440. 10.1121/1.4967506 . hal-01611021

**HAL Id: hal-01611021**

**<https://hal.science/hal-01611021v1>**

Submitted on 7 Nov 2019

**HAL** is a multi-disciplinary open access archive for the deposit and dissemination of scientific research documents, whether they are published or not. The documents may come from teaching and research institutions in France or abroad, or from public or private research centers.

L'archive ouverte pluridisciplinaire **HAL**, est destinée au dépôt et à la diffusion de documents scientifiques de niveau recherche, publiés ou non, émanant des établissements d'enseignement et de recherche français ou étrangers, des laboratoires publics ou privés.

## Source depth discrimination with a vertical line array

Ewen Conan, Julien Bonnel, Thierry Chonavel, and Barbara Nicolas

Citation: *The Journal of the Acoustical Society of America* **140**, EL434 (2016); doi: 10.1121/1.4967506

View online: <https://doi.org/10.1121/1.4967506>

View Table of Contents: <https://asa.scitation.org/toc/jas/140/5>

Published by the [Acoustical Society of America](#)

---

### ARTICLES YOU MAY BE INTERESTED IN

[Source depth discrimination: An evaluation and comparison of several classifiers](#)

*The Journal of the Acoustical Society of America* **138**, 1927 (2015); <https://doi.org/10.1121/1.4934068>

[Using the trapped energy ratio for source depth discrimination with a horizontal line array: Theory and experimental results](#)

*The Journal of the Acoustical Society of America* **142**, 2776 (2017); <https://doi.org/10.1121/1.5009449>

[Source depth estimation based on synthetic aperture beamforming for a moving source](#)

*The Journal of the Acoustical Society of America* **138**, 1678 (2015); <https://doi.org/10.1121/1.4929748>

[Use of mode subspace projections for depth discrimination with a horizontal line array: Theory and experimental results](#)

*The Journal of the Acoustical Society of America* **133**, 4019 (2013); <https://doi.org/10.1121/1.4804317>

[Array invariant-based source localization in shallow water using a sparse vertical array](#)

*The Journal of the Acoustical Society of America* **141**, 183 (2017); <https://doi.org/10.1121/1.4973812>

[Source localization in an ocean waveguide using supervised machine learning](#)

*The Journal of the Acoustical Society of America* **142**, 1176 (2017); <https://doi.org/10.1121/1.5000165>

---



CAPTURE WHAT'S POSSIBLE  
WITH OUR NEW PUBLISHING ACADEMY RESOURCES

Learn more 



# Source depth discrimination with a vertical line array

**Ewen Conan and Julien Bonnel**

*Laboratoire des Sciences et Techniques de l'Information, de la Communication et de la Connaissance, Unité Mixte de Recherche, Centre National de la Recherche Scientifique 6285, École Nationale Supérieure de Techniques Avancées, Bretagne, 2 rue François Verny, 29806 Brest Cedex 9, France*  
*ewen.conan@ensta-bretagne.org, julien.bonnel@ensta-bretagne.fr*

**Thierry Chonavel**

*Laboratoire des Sciences et Techniques de l'Information, de la Communication et de la Connaissance, Unité Mixte de Recherche, Centre National de la Recherche Scientifique 6285, Télécom Bretagne, 655 Avenue du Technopole, 29200 Plouzané, France*  
*thierry.chonavel@telecom-bretagne.eu*

**Barbara Nicolas**

*Université de Lyon, Centre de Recherche en Applications et Traitement de l'image pour la Santé, Centre National de la Recherche Scientifique, Unité Mixte de Recherche 5220, Inserm U1044, Institut National des Sciences Appliquées Lyon, Université Claude Bernard Lyon 1, France*  
*barbara.nicolas@creatis.insa-lyon.fr*

**Abstract:** Source depth estimation with a vertical line array generally involves mode filtering, then matched-mode processing. Because mode filtering is an ill-posed problem if the water column is not well-sampled, concerns for robustness motivate a simpler approach: source depth discrimination considered as a binary classification problem. It aims to evaluate whether the source is near the surface or submerged. These two hypotheses are formulated in terms of normal modes, using the concept of trapped and free modes. Decision metrics based on classic mode filters are proposed. Monte Carlo methods are used to predict performance and set the parameters of a classifier accordingly.

© 2016 Acoustical Society of America

[CCC]

**Date Received:** July 19, 2016     **Date Accepted:** October 25, 2016

## 1. Introduction

We address the problem of source depth discrimination in the context of underwater acoustics. The ability to differentiate surface sources from submerged ones could serve several applications, from anti-submarine warfare to marine biology. This paper focuses on the depth discrimination of a low-frequency monochromatic source, based on data acquired with a vertical line array (VLA) in a range-independent environment.

In this context, source localisation (range and depth estimation) is a well-known problem, and can be addressed with matched-mode processing methods. These are beam-forming methods operating in mode space, and thus require mode filtering to estimate modal amplitudes. However, when the water column is not well-sampled by the VLA, mode filtering becomes an ill-conditioned problem which can severely degrade localisation. Therefore, robustness concerns led us to consider source depth discrimination as a binary hypothesis test.

Source depth discrimination in such a context was originally addressed by Premus and coworkers.<sup>1-3</sup> Their work was based on the concept of trapped and free modes, which is particularly relevant in a downward-refracting shallow water environment. The tested hypotheses were that the deterministic part of the signal was due either only to free modes (surface source hypothesis) or only to trapped modes (submerged source hypothesis). The proposed decision metrics were energy ratios involving projections of the signal on different subspaces, associated with either the trapped or free modes.

In our work, we propose a new approach to source depth discrimination, where the tested hypotheses are formulated in terms of the source depth and involve a user-chosen discrimination depth. To test such hypotheses, we propose to use as a decision metric the proportion of energy borne by trapped modes, computed in mode space, and estimated with a classic modal filter.

The direct link between the hypothesis and the physical model allows evaluating the relevance of a decision metric through the use of Monte Carlo methods to

estimate receiver operating characteristics (ROCs). This enables us to compare the use of different mode filters to build our decision metric, which is illustrated on noisy data simulated on a VLA spanning only 50% of the water column, a configuration where a classic localisation scheme works poorly. Besides the choice of a decision metric, the performance computation also allows the choice of a decision threshold, according to an expected performance.

In Sec. 2, the normal-mode propagation model is presented, along with the physical concept of trapped and free modes. Section 3 presents source depth discrimination as a binary hypothesis test, and proposes decision metrics based on modal filtering. In Sec. 4, we use Monte Carlo performance evaluation to compare the proposed decision metrics.

## 2. The normal mode model

The normal mode representation describes the acoustic far field in the frequency domain as a finite sum of cylindrical propagative modes. For a monochromatic source at depth  $z_s$ , the pressure at receiver range  $r$  and depth  $z$  is

$$p(r, z) = X \frac{j e^{j\pi/4}}{\sqrt{8\pi\rho(z_s)}} \sum_{m=1}^M \psi_m(z_s) \psi_m(z) \frac{e^{-jr(k_{r_m} - j\alpha_m)}}{\sqrt{rk_{r_m}}}, \quad (1)$$

where  $k_{r_m}$ ,  $\alpha_m$ , and  $\psi_m$  are, respectively, the horizontal wavenumber, the attenuation coefficient, and the depth-dependent mode function for mode  $m$ ,  $\rho(z_s)$  is the water density at the source depth,  $M$  is the number of propagative modes, and  $X$  is the source complex amplitude at the considered frequency. Note that  $k_{r_m}$ ,  $\alpha_m$ , and  $\psi_m$  are frequency-dependent, but because we consider a monochromatic source, this dependence does not appear in our notations.

Equation (1) can be expressed as

$$p(r, z) = \sum_{m=1}^M \psi_m(z) d_m(r, z_s), \quad (2)$$

where the modal amplitude  $d_m(r, z_s)$  of the  $m$ th mode is

$$d_m(r, z_s) = X \frac{j e^{j\pi/4}}{\sqrt{8\pi\rho(z_s)}} \frac{e^{-jr(k_{r_m} - j\alpha_m)}}{\sqrt{rk_{r_m}}} \psi_m(z_s). \quad (3)$$

For an  $N$ -element VLA at range  $r$ , sampling the water column at depths  $z_1, \dots, z_N$ , the received signal can be expressed in vector notation,

$$\mathbf{p} = \begin{bmatrix} p(r, z_1) \\ \vdots \\ p(r, z_N) \end{bmatrix} = \begin{bmatrix} \psi_1(z_1) & \cdots & \psi_M(z_1) \\ \vdots & \ddots & \vdots \\ \psi_1(z_N) & \cdots & \psi_M(z_N) \end{bmatrix} \begin{bmatrix} d_1(r, z_s) \\ \vdots \\ d_M(r, z_s) \end{bmatrix} \quad (4)$$

$$\equiv \mathbf{\Psi} \mathbf{d}, \quad (5)$$

where  $\mathbf{\Psi}$  is the  $N \times M$  matrix of sampled mode functions (or observation matrix) and  $\mathbf{d}$  is the  $M \times 1$  vector of modal amplitudes. Note that  $\mathbf{\Psi}$  depends only on environment and array configuration, whereas  $\mathbf{d}$  depends on source position. Hence, source localisation with a VLA can be performed in two separate steps: mode filtering ( $\mathbf{d}$  estimation) then matched-mode processing.<sup>7</sup>

Mode filters are generally linear estimators in the form  $\hat{\mathbf{d}} = \mathbf{H} \mathbf{p}$ . Among the most common choices for  $\mathbf{H}$ , we find,<sup>4,5</sup>

- The matched filter (MF)  $\mathbf{H}_{\text{MF}} = \mathbf{\Psi}^H$ , where  $^H$  denotes conjugate transpose.
- The least-squares (LS) estimator (or pseudo-inverse)  $\mathbf{H}_{\text{LS}} = (\mathbf{\Psi}^H \mathbf{\Psi})^{-1} \mathbf{\Psi}^H$ .
- The regularised-least-squares (RLS) estimator  $\mathbf{H}_{\text{RLS}} = (\mathbf{\Psi}^H \mathbf{\Psi} + \beta \mathbf{I}_M)^{-1} \mathbf{\Psi}^H$ .
- The reduced-rank pseudo-inverse (RRPI)  $\mathbf{H}_{\text{RRPI}}$ , where the smallest singular values of  $\mathbf{\Psi}$  are set to zero before computing the pseudo-inverse.

The following developments rely on the fact that in a shallow water environment with a downward-refracting sound speed profile (SSP), surface sources generally couple poorly to low-order modes, a phenomenon referred to as mode trapping. As proposed by Premus and Helfrick,<sup>3</sup> we define as trapped the modes with phase speeds lower than the maximum sound speed in the water column. Non-trapped high-order modes, which can be excited by surface and submerged sources, are called free modes. Figure 1 illustrates the concept of mode-trapping. On the one hand, modal functions

show oscillatory depth-dependence where phase speed is higher than sound speed. On the other hand, trapped modes (modes 1 and 3 on Fig. 1) shows an exponential decay near the surface where phase speed is lower than sound speed, which limits coupling with surface sources.

This separation between trapped and free modes leads one to rewrite Eq. (5) in term of block matrices,

$$\mathbf{p} = \Psi \mathbf{d} \tag{6}$$

$$\equiv [\Psi_t \quad \Psi_f] \begin{bmatrix} \mathbf{d}_t \\ \mathbf{d}_f \end{bmatrix}, \tag{7}$$

where  $\Psi_t$  (respectively,  $\Psi_f$ ) is the matrix of sampled trapped (respectively, free) mode functions and  $\mathbf{d}_t$  (respectively,  $\mathbf{d}_f$ ) is the vector of trapped (respectively, free) modal amplitudes.

### 3. Depth discrimination

#### 3.1 Tested hypotheses

The problem is to determine, from a noisy VLA signal, whether the source responsible for the measured signal is a surface source or a submerged one. The problem will be addressed as a binary classification one, i.e., a choice between the two following hypotheses:

$$\begin{aligned} H_0 : z_s \leq z_{lim}, \\ H_1 : z_s > z_{lim}, \end{aligned} \tag{8}$$

where  $z_s$  is the source depth and  $z_{lim}$  the discrimination depth. Note that the  $z$ -axis is oriented downward, so  $H_0$  corresponds to surface sources and  $H_1$  to submerged ones. Moreover, the aim here is to discriminate surface and submerged sources, so the discrimination depth  $z_{lim}$  is set a few meters below the surface, typically between 5 and 10 m.

From a statistical signal processing point of view, tested hypotheses should be expressed in terms of measured signal distribution. Here, these distributions result from the physical model, and are completely determined by the environment and source frequency (on which depend  $k_{r_m}$ ,  $\alpha_m$ , and  $\psi_m$ ), source range and depth distributions, and noise distribution.

#### 3.2 Trapped energy ratio in mode space

Based on Eq. (3), we notice that, for a given environment, relative energy repartition in mode space depends mainly on source depth. Range affects it only through the attenuation coefficients  $\alpha_m$ , which are low for propagative modes. Thus, we use the concept of trapped and free modes to build the trapped energy ratio in mode space

$$R_d = \frac{\|\mathbf{d}_t\|^2}{\|\mathbf{d}\|^2}, \tag{9}$$

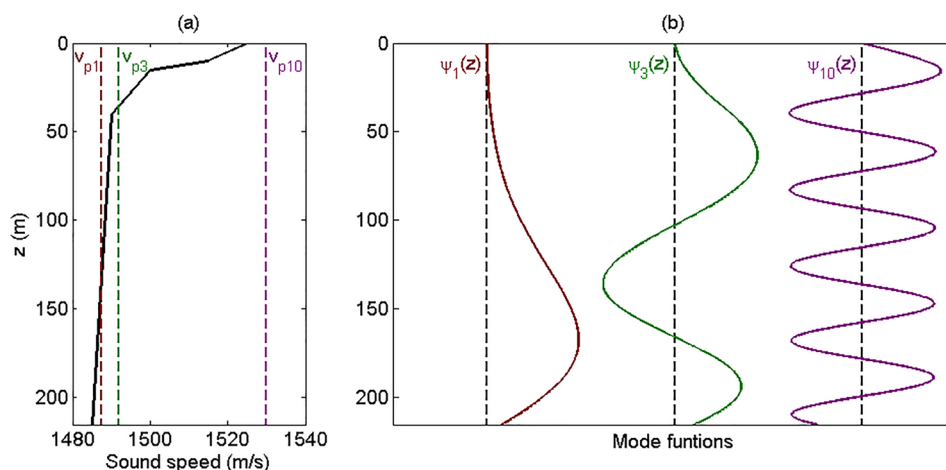


Fig. 1. (Color online) Diagram illustrating the concept of mode trapping. (a) Sound speed profile (solid line) and phase speed of modes 1, 3, 10 (dashed lines). (b) Modal depth functions for modes 1, 3, 10.

which depends mainly on source depth. Figure 2 shows the evolution of the trapped energy ratio  $R_d$  with source depth in a shallow water environment, for different source ranges. These curves are valid for the given environment and frequency, but similar behaviours are observed with other downward-refracting SSP: an oscillatory plateau in the main part of the water column, decreasing near the boundaries, with lower value at the surface than at seabed. It is thus considered representative, and is used in the subsequent reasoning.

The behaviour of trapped energy ratio, exhibited on Fig. 2, makes it a pertinent physical quantity for source depth discrimination. In particular, if we neglect attenuation ( $\alpha_m=0$ ), the trapped energy ratio depends only on source depth, not on source range. Thus, for discrimination depth close enough to the surface (lower than 10 m on the example of Fig. 2), the hypotheses on source depth in Eq. (8) are equivalent to the following hypotheses on trapped energy ratio:

$$\begin{aligned} H_0 : R_d(z_s) &\leq R_{lim} \equiv R_d(z_{lim}), \\ H_1 : R_d(z_s) &> R_{lim} \equiv R_d(z_{lim}). \end{aligned} \tag{10}$$

In the presence of viscous attenuation, the trapped energy ratio globally increases with distance, because trapped modes are lower-order modes, therefore less attenuated. However, the general shape of the curve is preserved, which still allows depth discrimination.

### 3.3 Decision metrics

The previous considerations lead us to use an estimation of the trapped energy ratio as a decision metric for source depth discrimination. An intuitive way to estimate this ratio from the measured pressure is to use the output  $\hat{\mathbf{d}} = [\hat{\mathbf{d}}_t^T \hat{\mathbf{d}}_f^T]^T$  of a mode filter,

$$\hat{R}_d = \frac{\|\hat{\mathbf{d}}_t\|^2}{\|\hat{\mathbf{d}}\|^2}. \tag{11}$$

Note that such an estimate depends on the choice of the mode filter, which affects  $\hat{\mathbf{d}}$ . Therefore, each particular mode filter defines a particular decision metric.

The discrimination is done by comparing such a decision metric to a decision threshold  $\eta$ ,

$$\begin{aligned} \hat{R}_d \leq \eta &\rightarrow H_0, \\ \hat{R}_d > \eta &\rightarrow H_1. \end{aligned} \tag{12}$$

The performance of such a classifier is affected by the choice of the decision threshold  $\eta$ . Thus this choice can be made according to expected performance (generally a given false alarm rate) with the help of the receiver operating characteristic (ROC).

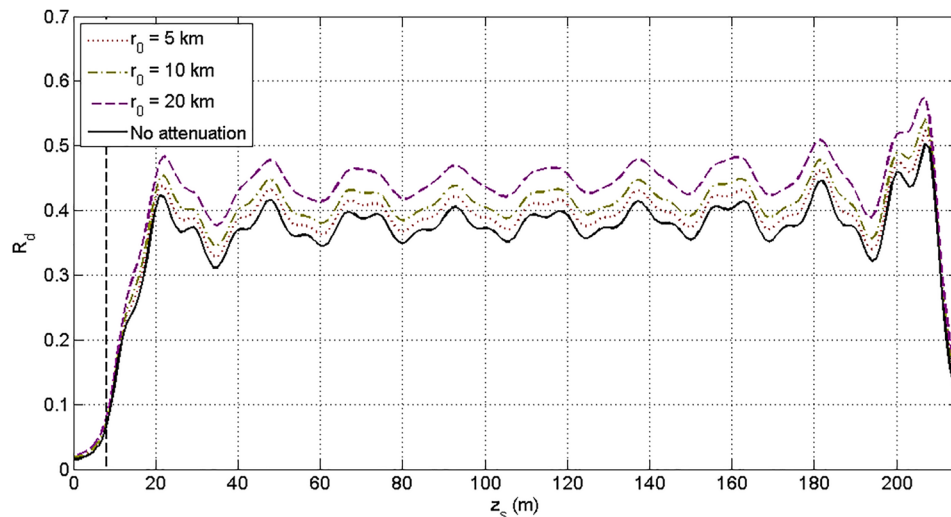


Fig. 2. (Color online) Evolution of the trapped energy ratio with source depth in a shallow water environment, for different source ranges. The sound speed profile and mode functions are the same as in Fig. 1. The solid line is the trapped energy ratio without attenuation, which is independent of source range. The vertical dashed lines indicate the discrimination depth  $z_{lim}$  chosen in Sec. 4.

Compared to matched-mode processing depth estimation, considering energy in mode groups rather than individual modal amplitudes allows for better robustness against modal filtering error. Indeed, mode leakage affects mainly adjacent modes, so that the bias on a mode estimate is mainly due to modes of the same group.

Compared to the decision metric previously proposed by Premus and Helfrick,<sup>3</sup> the main difference is that energy ratio is here computed in mode space, whereas they use projections and compute some energy ratio in phone space. Working in mode space should make the metrics less sensitive to modal interferences on the array, and therefore to source range. A more minor difference is that the ratio proposed here compares trapped energy to the total energy, whereas the ratio of Premus and Helfrick compares trapped energy to free energy. As a result, our ratio is the proportion of energy borne by trapped modes.

The main limitation of the proposed approach resides in the use of trapped and free modes: it is valid for a low-frequency source (so that modal propagation is an appropriate model) in a downward-refracting SSP (so that the first modes are trapped).

#### 4. Performance evaluation

##### 4.1 General methodology

The propagation hypotheses and classification problem being rigorously defined, it is possible to evaluate a classifier's performance with classical binary classification tools and Monte Carlo methods. As some tools from detection theory will be used to evaluate binary classifiers' performance, it is necessary to specify that detection refers here to the submerged source hypothesis  $H_1$ . Hence, the detection rate  $P_D$  is the probability for a submerged source to be correctly classified (as a submerged source), and the false alarm rate  $P_{FA}$  is the probability for a surface source to be classified as submerged. Then, the probability for a submerged source to be classified as a surface source is  $1 - P_D$  and the probability for a surface source to be correctly classified is  $1 - P_{FA}$ .

For a given classifier in given environmental conditions, Monte Carlo methods are used to evaluate the detection and false alarm rates  $P_D$  and  $P_{FA}$ . In the case where the classifier relies on a comparison of a data-based metric with a decision threshold  $\eta$  [see Eq. (12)], a receiver operating characteristic (ROC) can give a general view of the metric's relevance and help to choose an appropriate decision threshold, based on expected performance.

An example of performance evaluation is conducted hereafter, and ROC curves obtained with different decision metrics are presented.

##### 4.2 Hypotheses specification

First, we have to specify the tested hypotheses so that the distribution of measured signal under each hypothesis is completely determined.

The tested environment is 215-m deep and has the sound speed profile presented in Fig. 1. We consider a fluid bottom, with a sound speed of 1800 m/s and attenuation of 0.1 dB/ $\lambda$ . The source frequency is chosen to be 150 Hz. Mode functions, wavenumbers and attenuation coefficients are numerically computed with KRAKEN (Ref. 6): there are 24 propagative modes, 9 of which are trapped. The chosen array is a 30-hydrophone VLA with a 3.7-m inter-element spacing, spanning only 50% of the water column. Such a configuration corresponds to an observation matrix  $\Psi$  whose conditioning number is  $1.4e8$ , so modal filtering is expected to work poorly in presence of noise.

Discrimination depth is set at 8 m. Source depths are randomly drawn from a uniform distribution between  $z_{lim}$  and the appropriate water column boundary (surface for  $H_0$ , bottom for  $H_1$ ). Source ranges are randomly drawn from a uniform distribution between 1 and 20 km.

For generality purpose, we consider a spatially white noise, following a complex circular normal distribution. The signal-to-noise ratio (SNR) is set to 5 dB. For the noised VLA signal  $\mathbf{p} = \Psi\mathbf{d} + \mathbf{w}$ , SNR is given by

$$SNR = 10 \log_{10} \frac{\|\Psi\mathbf{d}\|^2}{E\{\|\mathbf{w}\|^2\}}. \quad (13)$$

##### 4.3 Decision metrics

As we stated before, the estimation of the trapped energy ratio in Eq. (11) depends on the choice of a particular mode filter. Thus, the four mode filters presented in Sec. 2 define four distinct decision metrics. We consider these four metrics, and the one proposed by Premus and Helfrick.<sup>3</sup>

Because RRPI and RLS modal filters are tunable, the corresponding decision metrics are too. Their parameters are set to maximise the area under the ROC curve. For the RLS approach,  $\beta$  is set to 0.05. For the RRPI approach, the rank is reduced from 24 to 14. The decision metric of Premus and Helfrick<sup>3</sup> also involves rank reduction, to remove overlap between subspaces of trapped and free modes. The maximal area under the ROC curve is reached with the original trapped subspace dimension (9) and a dimension of the free subspace reduced from 15 to 10.

#### 4.4 Results

Figure 3 shows obtained ROC curves for the four decision metrics based on estimation of the trapped energy ratio, and the decision metric of Premus and Helfrick. Monte Carlo methods involved  $5e5$  realisations of the pressure signal under each hypothesis.

The best performances are obtained with the RLS-based approach. Because the RLS filter can be identical to the MF or the LS filters for particular values of  $\beta$ , both the latter filters were expected to give poorer results than the RLS approach with an optimised  $\beta$ .

Although  $\Psi$  is not orthogonal and so the matched filter is a biased estimator, the MF-based classifier happens to give good results in this case. In fact, the aim here is not to estimate modal amplitudes themselves, but the repartition of energy between two groups of modes. Then, the matched filter seems particularly appropriate in the extent that  $\Psi^H\Psi$  is nearly an order-2 band matrix in the present case.

Because of the high conditioning number and noise level, the classifier based on LS filter (or pseudo-inverse) follow the non-discrimination line  $P_D(\eta) = P_{FA}(\eta)$ , i.e., a random guess would be as efficient. Concerning the RRPI approach, rank-reduction before computing the pseudo-inverse allows better performance, but not as good as the RLS approach.

In this configuration, the decision metric of Premus and Helfrick<sup>3</sup> gives nearly the same results as the RRPI approach. Note that the definition of the depth discrimination problem of Premus and Helfrick is slightly different than ours, as an equivalent of our discrimination depth  $z_{lim}$  is never explicitly given. As a result, the comparison with the other decision metrics is not straightforward, because the computed performance depends on the choice of  $z_{lim}$ . One could think our choice of  $z_{lim}$  is not appropriate for this decision metric, but similar results were observed for different values of  $z_{lim}$ .

Another type of classifier based on matched-mode processing<sup>7</sup> has been implemented and evaluated. Matched-mode processing estimates the source depth by matching simulated replicas to the filtered modes. Comparing this estimated depth to the discrimination depth  $z_{lim}$  is a simple way to choose between the two hypotheses. With any of the mode filters previously described, such a classifier yields false alarm rates higher than 30% in these conditions, whereas the method defined by Eq. (11) and Eq. (12) allows for low false alarm rates while achieving reasonable detection rates (except for the LS mode filter). This highlights the interest of the source depth discrimination approach, compared to depth estimation.

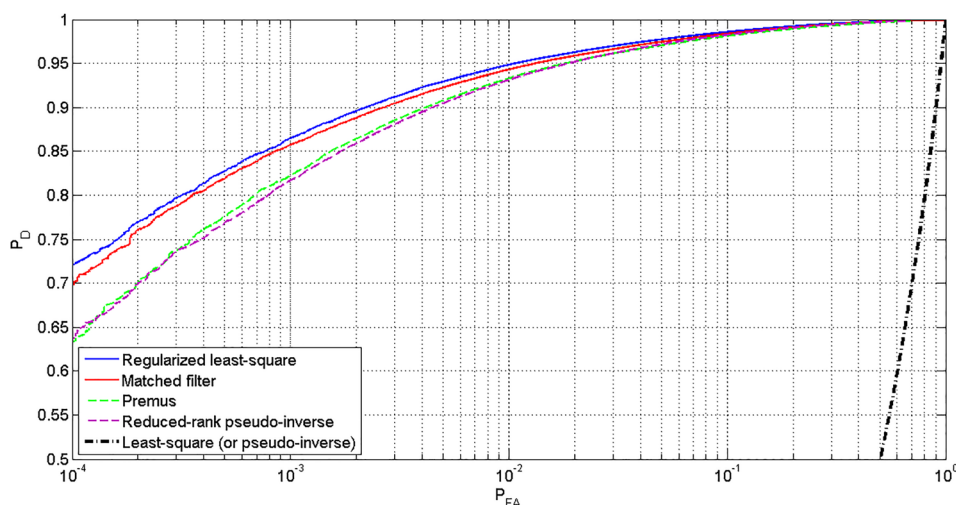


Fig. 3. (Color online) ROC curves for decision metrics based on classic mode filters and decision metric of Premus and Helfrick. The parameters of tunable decision metrics were set to maximise the area under the ROC curve.



The results presented here allow one to choose a decision threshold  $\eta$  to which the decision metric is compared. This choice results of a compromise between false alarm and true detection. Note that as the ROC is a parametric curve, with parameter  $\eta$ , the value of  $\eta$  corresponding to a certain compromise cannot be read directly on Fig. 3.

## 5. Conclusion

A new approach to depth discrimination has been proposed, as well as simple decision metrics based on classic mode filters. Monte Carlo methods were used to evaluate the performance of a classifier in given conditions. In the case where the classification is done by comparing a decision metric with a threshold, the choice of this threshold can be based on an expected false alarm rate.

Note that performance evaluation is performed in some given conditions (which define the tested hypotheses). For each practical case, the evaluation and comparison of the decision metrics should be performed on simulated data, in order to choose the best metric and a relevant decision threshold. After this theoretical study, the discrimination can be performed on the real data.

The method has been tested on simulated data for a vertical array spanning only half of the water column in a shallow water environment. According to the ROC analysis, the use of the regularised-least square mode filter to estimate the trapped energy ratio gives the better discrimination results. Furthermore, the proposed method allows for lower false alarm rate than a decision based on matched-mode processing.

## References and links

- <sup>1</sup>V. E. Premus, J. Ward, and C. D. Richmond, "Mode filtering approaches to acoustic source depth discrimination," in *Proceedings of the 38th Asilomar Conference on Signals, Systems and Computers* (2004), pp. 1415–1420.
- <sup>2</sup>V. E. Premus and D. Backman, "A matched subspace approach to depth discrimination in a shallow water waveguide," in *Proceedings of the 41st Asilomar Conference on Signals, Systems and Computers* (2007), pp. 1272–1276.
- <sup>3</sup>V. E. Premus and M. N. Helfrick, "Use of mode subspace projections for depth discrimination with a horizontal linear array," *J. Acoust. Soc. Am.* **133**(6), 4019–4031 (2013).
- <sup>4</sup>J. R. Buck, J. C. Preisig, and K. E. Wage, "A unified framework for mode filtering and the maximum a posteriori mode filter," *J. Acoust. Soc. Am.* **103**(4), 1813–1824 (1998).
- <sup>5</sup>J. C. Papp, J. C. Preisig, and A. K. Morozov, "Physically constrained maximum likelihood mode filtering," *J. Acoust. Soc. Am.* **127**(4), 2385–2391 (2010).
- <sup>6</sup>M. B. Porter, *The Kraken Normal Mode Program*, technical report, DTIC document, 1992.
- <sup>7</sup>T. C. Yang, "A method of range and depth estimation by modal decomposition," *J. Acoust. Soc. Am.* **82**(5), 1736–1745 (1987).